

Crystal and magnetic structure of the perovskites La_2MTiO_6 ($\text{M} = \text{Co}, \text{Ni}$)

Elizabeth Rodríguez,^a María Luisa López,^{*a} Javier Campo,^b María Luisa Veiga^a and Carlos Pico^a

^aDepartamento de Química Inorgánica I, Facultad de Ciencias Químicas, Universidad Complutense, 28040 Madrid, Spain. E-mail: marisal@quim.ucm.es

^bInstitut Max Von Laue–Paul Langevin (ILL), 38042 Grenoble Cedex 9, France

Received 11th March 2002, Accepted 1st May 2002

First published as an Advance Article on the web 6th August 2002

The crystal structures of the perovskites La_2MTiO_6 ($\text{M} = \text{Co}$ and Ni) were determined on the basis of powder neutron diffraction data collected at room temperature. Refinements of the data showed that these compounds have monoclinic symmetry, space group $P2_1/n$, and the common structure is a perovskite-type with a partially ordered arrangement of $\text{M}(\text{II})$ and $\text{Ti}(\text{IV})$ cations on the 6-coordination sites.

Magnetic structures of type II have been determined from neutron diffraction data collected at 1.5 K and it was found that there was a long range antiferromagnetic ordering where only the M^{2+} ions are responsible for their magnetic properties. The antiferromagnetic ordering is explained by means of a propagation vector [$k = 1/2, 0, 1/2$] and the respective magnetic moments at 1.5 K are $2.88 \mu_B$ for Co and $2.05 \mu_B$ for Ni.

Introduction

Perovskite-type oxides of the transition elements have been extensively studied since they present interesting magnetic and transport properties. Famous examples are superconducting mixed-valent copper oxides and the mixed-valent manganese perovskites exhibiting giant magnetoresistance.¹ In either case the special physical properties are strongly related to charge-ordering phenomena.

Mixed oxides of stoichiometry LnMO_3 show a great variety of symmetries and magnetic structures. The different symmetries adopted by these compounds are governed by the ionic radii size of the cations which are occupying A and B sublattices in the perovskite structures. Some of these compounds show antiferromagnetic transitions at low temperature. For instance, the spin arrangements adopted in LaCrO_3 ² and LaFeO_3 ³ show a type G ordering whilst LaMnO_3 ³ present a type A ordering. Therefore, it is particularly interesting to consider LnNiO_3 ^{4,5} for which an unusual antiferromagnetic structure was found, with $k = [1/2, 0, 1/2]$ relative to the orthorhombic crystal cell. On the other hand, YNiO_3 ⁶ is monoclinic due to a charge disproportion where NiO_6 octahedra are alternated with expanded (Ni1) and contracted (Ni2) Ni–O bonds. The magnetic structure, with unequal moments at Ni1 and Ni2 octahedra, has been reported as being $k = [1/2, 0, 1/2]$ in this case. Moreover, regarding the fact that the Ni2 positions tend towards a diamagnetic state, the Ni1–Ni1 magnetic interactions between second nearest neighbours are expected to be greater compared to those between the nearest neighbours, that is, the Ni1–Ni2 atoms.

The crystal structures and magnetic properties of perovskite-related materials with the double formula $\text{A}_2\text{BB}'\text{O}_6$ depend upon the size and electronic structure of the transition metal cations B and B'. If the two species are of similar size and charge they are likely to be distributed over the 6-coordinate sites in a disordered manner; otherwise they arrange themselves in an alternate manner thus increasing the size of the unit cell. The presence of cation disorder on the B sublattice gives rise to unusual magnetic properties, for example, competing superexchange interactions lead to a spin–glass behaviour in $\text{Sr}_2\text{FeRuO}_6$ and BaLaNiRuO_6 .⁷ By contrast, in ordered perovskites

such as $\text{Ba}_2\text{NdRuO}_6$ ⁸ and $\text{Sr}_2\text{HoRuO}_6$ ⁹ a long range antiferromagnetic ordering involving Ru^{5+} and Nd^{3+} , or Ho^{3+} , respectively, were found. On the other hand, the magnetically more dilute compounds such as SrLaFeSnO_6 and SrLaNiSbO_6 ¹⁰ show disordered and ordered arrangements of B cations, respectively, and are antiferromagnetically ordered at low temperatures.

This paper describes the crystal and magnetic structures that explain the magnetic behaviour of La_2MTiO_6 , ($\text{M} = \text{Co}$ and Ni) as revealed by neutron diffraction experiments.

Experimental

Polycrystalline samples La_2MTiO_6 ($\text{M} = \text{Co}$ and Ni) were prepared by the “liquid mix” technique.¹¹ This technique is based on the formation of metallic complex from concentrated solutions of polyfunctional organic acids and either salts or oxides of soluble cations for mixed oxide formation. Stoichiometric amounts of $\text{C}_{10}\text{H}_{14}\text{O}_5\text{Ti}$, $\text{La}(\text{NO}_3)_3 \cdot 6\text{H}_2\text{O}$ and $\text{M}(\text{NO}_3)_2 \cdot 6\text{H}_2\text{O}$ (4 g of these reagents) were dissolved in citric acid until saturation (10 g of citric acid and some drops of HNO_3), a transparent liquid solution being obtained. In order to solidify the liquid solution it is necessary to add a diol which increases the solution viscosity due to the formation of ester-type three-dimensional polymers.¹² When the diol reacts with the citric solution a resin is formed, thus avoiding formation of partial segregations which could modify the homogeneity of the solution. In this way 4 ml of ethylene glycol (3% v/v) was added to the above citric solution. Evaporation of the solution obtained gave a vitreous intermediate polymer containing all the cations in the desired stoichiometric amounts. The excess of nitric acid was boiled off and the organic resin was slowly decomposed by heating up to 513 K for 48 h, in an alumina crucible, followed by a further thermal treatment at 723 K for 72 h, a homogeneous cationic distribution being obtained. Finally, the samples were heated in air at temperatures ranging between 1073 and 1173 K for several days.

Neutron powder diffraction patterns were recorded at room temperature on the D1A high-resolution powder diffractometer ($\lambda = 1.9110 \text{ \AA}$) at the Institut Laue-Langevin (Grenoble, France). The angular range $5 < 2\theta < 160^\circ$ was scanned with a

step size of 0.05°. The sample were contained in 16 mm diameter vanadium cans. The Rietveld profile analysis method¹³ was applied to refine the neutron diffraction data. A multidetector D1B powder diffractometer with a wavelength of 2.52 Å was used for thermal patterns in the temperature range 1.5–300 K.

Magnetic measurements were obtained in a SQUID magnetometer (Quantum Design, MPMS-XL model) with a sensitivity of 10⁻¹⁰ emu in the temperature range 2–300 K, applying a field of 1000 Oe.

Results and discussion

1. Crystal structure

La₂NiTiO₆ has previously been described¹² from XRD as an orthorhombic perovskite and the neutron powder diffraction data collected at room temperature on La₂MTiO₆ (M = Co, Ni) were consistent with the adoption of a monoclinic distorted cell, whose parameters were *ca.* $\sqrt{2}a_p \times \sqrt{2}a_p \times 2a_p$, where a_p is the unit cell parameter of a simple cubic perovskite. But our attempts to refine the neutron diffraction patterns in the space group *Pbnm* were unsuccessful and we therefore lowered the symmetry to monoclinic, in the space group *P2₁/n*, which does

permit ordering of M²⁺ and Ti⁴⁺ cations over the 6-coordinate sites of the structure. The contrast in scattering lengths for Ni or Co (10.3 and 2.5 fm) and for Ti (-3.3 fm) allow the distribution of these cations over 2c and 2d sites to be determined with precision. The final values of the refined parameters are listed in Table 1 and the corresponding bond lengths and bond angles in Table 2. The observed and calculated neutron diffraction patterns are shown in Fig. 1.

The M/Ti arrangement over the two crystallographically distinct B sites was allowed to vary, with the constraint that the 1 : 1 composition ratio was maintained. The results indicate that 74% of Co and 86% of Ni are occupying the 2c sites (Table 1). Therefore, the crystal structures of the title compounds have a partially ordered arrangement of cations on the 6-coordinate sites. The difference in charge between M²⁺ and Ti⁴⁺ will be relatively small and the move towards an ordered structure is more likely to be determined by the size difference between the two cations (*i.e.*, $r(\text{Ni}^{2+}) = 0.69 \text{ \AA}$, $r(\text{Co}^{2+}) = 0.745 \text{ \AA}$, $r(\text{Ti}^{4+}) = 0.605 \text{ \AA}$). The average length of the B–O bonds (Table 2) is similar to the value of 1.99 Å for the Ti–O bonds in La_{2/3}Li_{0.11}Ti₂O₆,¹⁴ where the mean B–O bond lengths approach that of 2.03 Å and 2.04 Å found for Co–O and Ni–O in other mixed oxides.¹²

Table 1 Lattice parameters, atomic coordinates, and conventional discrepancy factors from Rietveld refinement of neutron diffraction data obtained at 300 and 1.5 K (bold) for La₂MTiO₆

M = Co						
<i>a</i> /Å	<i>b</i> /Å	<i>c</i> /Å	β /°	<i>V</i> /Å ³		
5.5621(7)	5.5667(7)	7.8502(8)	89.86(1)	243.06(5)		
5.5538(5)	5.5641(5)	7.8388(7)	89.87(1)	242.23(4)		
Atom	Site	<i>x</i>	<i>y</i>	<i>z</i>	Occ	β /Å ²
La	4e	0.5064(1)	0.5293(8)	0.2506(2)	1.00	0.81(7)
		0.5069(1)	0.5326(6)	0.2499(1)		0.32(7)
Ti ^a	2d	½	0	0	0.74(1)	0.34(9)
						0.15(8)
Co ^a	2c	0	½	0	0.74(1)	1.79(9)
						1.51(9)
O1	4e	0.2038(1)	0.2126(2)	-0.0428(1)	1.00	0.39(2)
		0.2049(1)	0.2059(1)	-0.0410(1)		0.72(2)
O2	4e	0.2688(2)	0.7229(2)	-0.0306(1)	1.00	1.72(2)
		0.2769(1)	0.7331(2)	-0.0343(1)		0.74(2)
O3	4e	0.4245(1)	0.9898(1)	0.2518(2)	1.00	0.37(1)
		0.4225(1)	0.9886(1)	0.2464(1)		0.03(1)
<i>R_p</i> : 18.1, <i>R_wp</i> : 16.2, <i>R_B</i> : 5.88						
<i>R_p</i> : 17.0 , <i>R_wp</i> : 16.1 , <i>R_B</i> : 5.80 , <i>R_M</i> : 17.2 ($\mu_x = 0.05(5)$, $\mu_z = 2.88(1)$)						
M = Ni						
<i>a</i> /Å	<i>b</i> /Å	<i>c</i> /Å	β /°	<i>V</i> /Å ³		
5.5545(6)	5.5512(5)	7.8341(8)	90.08(2)	241.55(4)		
5.5446(5)	5.5458(5)	7.8232(7)	90.10(1)	240.56(3)		
Atom	Site	<i>x</i>	<i>y</i>	<i>z</i>	Occ	β /Å ²
La	4e	0.5080(1)	0.5303(8)	0.2586(2)	1.000	0.53(7)
		0.5069(1)	0.5335(6)	0.2501(2)		0.07(1)
Ti ^a	2d	½	0	0	0.86(2)	1.80(6)
						0.07(4)
Ni ^a	2c	0	½	0	0.86(2)	1.39(1)
						0.59(1)
O1	4e	0.2286(2)	0.2173(3)	-0.0269(2)	1.000	2.50(3)
		0.2253(2)	0.2162(3)	-0.0330(2)		2.15(8)
O2	4e	0.2945(2)	0.7106(2)	-0.0376(1)	1.000	0.66(2)
		0.2922(2)	0.7107(2)	-0.0362(1)		0.25(2)
O3	4e	0.4266(2)	0.9928(1)	0.2411(1)	1.000	0.69(1)
		0.4274(1)	0.9910(9)	0.2378(1)		0.60(1)
<i>R_p</i> : 17.6, <i>R_wp</i> : 17.0, <i>R_B</i> : 5.84						
<i>R_p</i> : 17.0 , <i>R_wp</i> : 16.6 , <i>R_B</i> : 5.05 , <i>R_m</i> : 32.3 ($\mu_x = -0.36(1)$, $\mu_z = 2.02(1)$)						
^a Occ M (2d) = 1-occ Ti; Occ Ti (2c) = 1-occ M						

Table 2 Bond lengths (Å) and angles (°) for La₂MTiO₆

M = Co 300 K					
La–O1	2.768(1)	La–O2	2.792(2)	La–O3	2.604(8)
	2.703(1)		2.645(1)		2.408(1)
	2.378(1)		2.551(1)	Mean:	2.606
Ti–O1	1.989(1) × 2	Co–O1	2.057(1) × 2		
Ti–O2	1.958(1) × 2	Co–O2	2.023(1) × 2		
Ti–O3	1.995(1) × 2	Co–O3	2.021(1) × 2		
Mean:	1.981		2.033		
Ti–O1–Co:	154.1(6)				
Ti–O2–Co:	159.9(7)				
Ti–O3–Co:	155.6(6)				
M = Co 1.5 K					
La–O1	2.740(1)	La–O2	2.802(3)	La–O3	2.580(3)
	2.711(3)		2.612(4)		2.397(1)
	2.380(1)		2.545(2)	Mean:	2.596
Ti–O1	2.026(1) × 2	Co–O1	2.019(1) × 2		
Ti–O2	1.953(1) × 2	Co–O2	2.029(2) × 2		
Ti–O3	1.979(2) × 2	Co–O3	2.036(1) × 2		
Mean:	1.986		2.028		
Co–O1–Ti:	153.5(9)				
Co–O2–Ti:	159.7(7)				
Co–O3–Ti:	154.9(4)				
M = Ni 300 K					
La–O1	2.720(2)	La–O2	2.758(2)	La–O3	2.607(8)
	2.695(2)		2.697(1)		2.420(1)
	2.493(2)		2.445(1)	Mean:	2.604
Ti–O1	1.941(1)	Ni–O1	2.034(1)		
Ti–O2	1.990(1)	Ni–O2	2.032(1)		
Ti–O3	1.933(1)	Ni–O3	2.071(1)		
Mean:	1.955		2.045		
Ti–O1–Ni:	161.4(2)				
Ti–O2–Ni:	155.3(1)				
Ti–O3–Ni:	155.4(6)				
M = Ni 1.5 K					
La–O1	2.755(2)	La–O2	2.718(1)	La–O3	2.577(8)
	2.502(2)		2.702(3)		2.421(2)
	2.651(2)		2.425(2)	Mean:	2.594
Ti–O1	1.955(1) × 2	Ni–O1	2.026(1) × 2		
Ti–O2	1.995(2) × 2	Ni–O2	2.018(1) × 2		
Ti–O3	1.905(2) × 2	Ni–O3	2.090(1) × 2		
Mean:	1.951		2.044		
Ti–O1–Ni:	159.2(5)				
Ti–O2–Ni:	156.4(1)				
Ti–O3–Ni:	155.5(3)				

2. Magnetic structure

The temperature dependence of the molar magnetic susceptibilities for La₂MTiO₆ (M = Co and Ni) are shown in Figs. 2 and 3 respectively. It can be observed that the susceptibility obeys a Curie–Weiss law between 300 and 100 K for both compounds. The magnetic moments calculated for this temperature range are 5.06 μ_B for the Co compound and 3.12 μ_B for the Ni one. The magnetic moments obtained agree fully with those expected for the octahedral field term ⁴T₁ (for Co²⁺) or ³A₂ (for Ni²⁺). Around 25 K a maximum appears which suggests antiferromagnetic ordering for both samples.

We shall focus on the magnetic structure in order to interpret the above results. Neutron diffraction patterns on the D1B diffractometer from 1.5 K to room temperature are shown in Fig. 4 for La₂CoTiO₆ and these data were used to follow the thermal evolution of the main magnetic reflections. Diffraction patterns revealed the presence of very weak reflections at about 20 K that can be indexed with integer indices in a lattice with double *a* and *c* axes relative to the monoclinic crystal cell; these superlattice reflections are defined by the wave vector $\mathbf{k} = [\frac{1}{2}, 0, \frac{1}{2}]$. In order to confirm their nature, neutron diffraction patterns on the D1A diffractometer ($\lambda = 1.911$ Å) were registered at 1.5 K and are given in Fig. 5. It is interesting to note the appearance of identical magnetic features at this temperature that reveal the same magnetic ordering in both compounds.

We tried to determine the magnetic structures of La₂CoTiO₆ and La₂NiTiO₆ from the data diffraction collected at 1.5 K

using the analysis FULLPROF program. Preliminary refinements of the crystal structure indicate that no major change had occurred on cooling and the cation distributions over the sites B and B' was therefore held constant at the previously determined ratio during analysis of the low temperature data. Simultaneous refinements of the crystal and magnetic structures then resulted in the structural parameters listed in Table 1 (bold), with the corresponding bond lengths in Table 2 (in bold) and the observed and calculated diffraction patterns drawn in Fig. 6 for both compounds. A satisfactory agreement for the magnetic intensities was obtained for the collinear magnetic structure sketched in Fig. 6 (R_{mag} (Co) = 16 and R_{mag} (Ni) = 32) where, consistent with the above magnetic propagation vector, the coupling between paramagnetic ions are AFM in the *a*–*c* plane and FM parallel to the *b* axis. As shown in Fig. 6, all magnetic moments lie in the *a*–*c* plane, with a deviation of ±1° and ±10°, respectively, from the *z* axis. The best magnetic matches correspond to moment values of 2.88 μ_B and 2.05 μ_B at Co²⁺ and Ni²⁺, respectively. These values are near to those expected from $2S = 3 \mu_B$ for Co²⁺ and $2S = 2 \mu_B$ for Ni²⁺ and the components are also given in Table 1.

The magnetic structures of both compounds are consistent with the presence of a long-range cation order. The partial ordering of M²⁺ and Ti⁴⁺ into B sites of the perovskite reduces the number of magnetic nearest-neighbour pairs (separation between nearest-neighbour (nn), *a*_p), whilst increasing the number of magnetic next-nearest-neighbour (nnn) pairs (separation $\sqrt{2}a_p$).

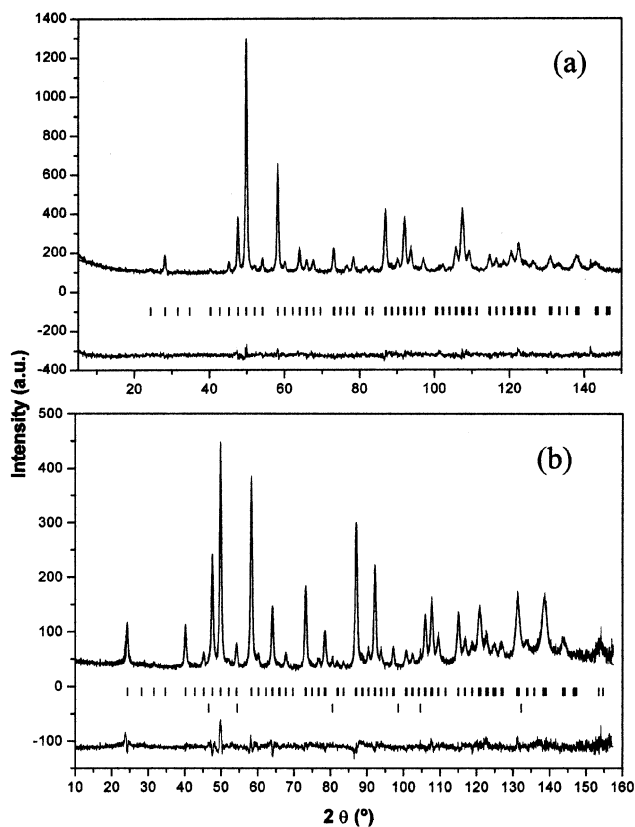


Fig. 1 Neutron powder diffraction patterns obtained at 300 K. Experimental, calculated, and difference diagrams are plotted for (a) $\text{La}_2\text{CoTiO}_6$ and (b) $\text{La}_2\text{NiTiO}_6$.

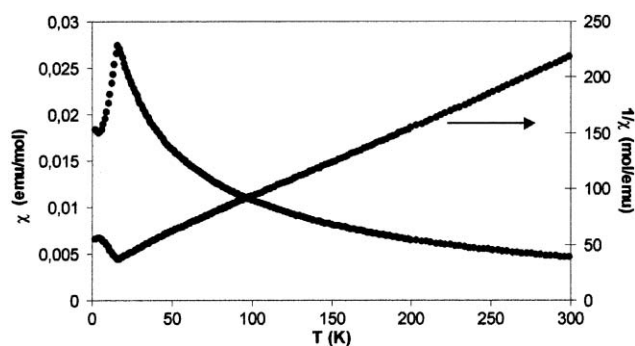


Fig. 2 Variation of χ and χ^{-1} vs. temperature for $\text{La}_2\text{CoTiO}_6$.

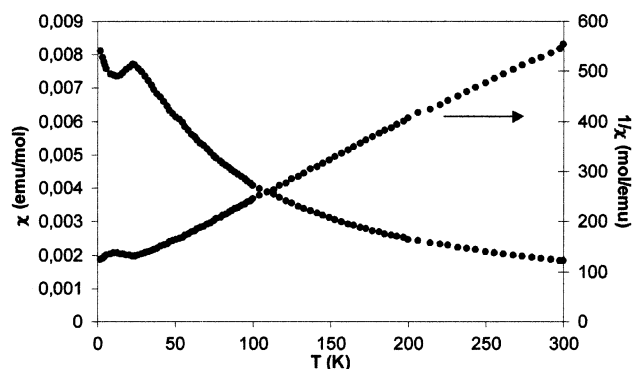


Fig. 3 Variation of χ and χ^{-1} vs. temperature for $\text{La}_2\text{NiTiO}_6$.

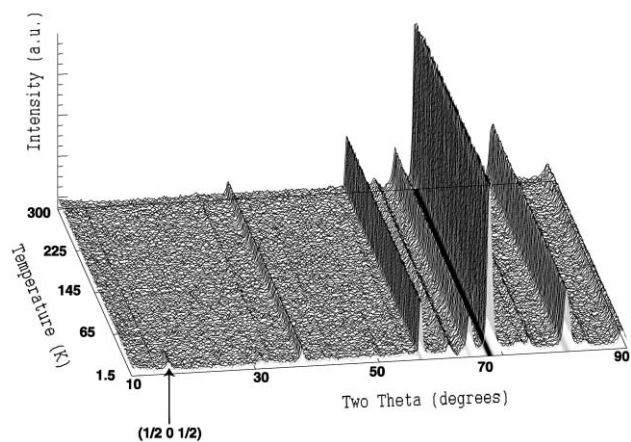


Fig. 4 Neutron thermodiffractogram of the compound $\text{La}_2\text{CoTiO}_6$ between 1.5 and 300 K and angular range 10° – 90° . At $T_N = 20$ K, some magnetic peaks become visible.

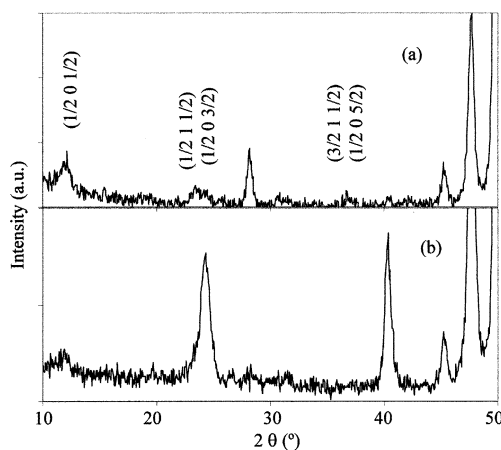


Fig. 5 Detail of main magnetic reflections at 1.5 K for (a) $\text{La}_2\text{CoTiO}_6$ and (b) $\text{La}_2\text{NiTiO}_6$.

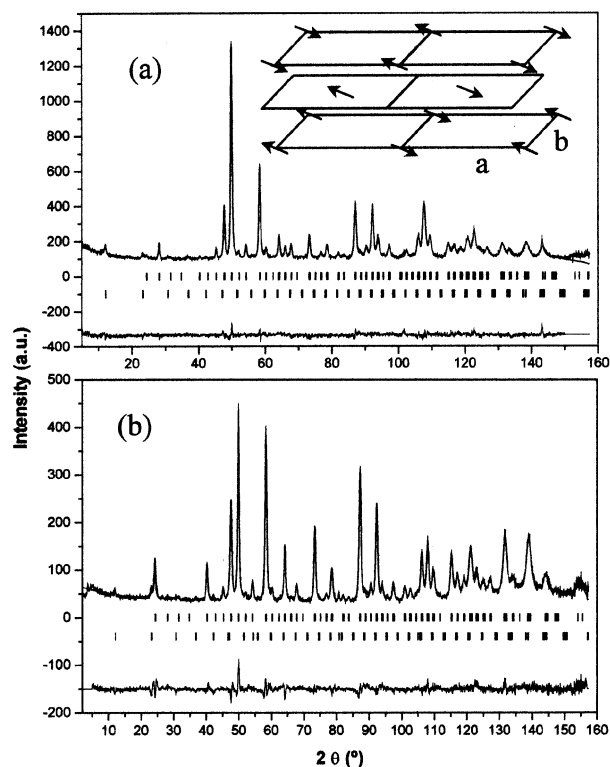


Fig. 6 Neutron powder diffraction patterns obtained at 1.5 K. Experimental, calculated, and difference diagrams are plotted. Vertical marks show the allowed structural and magnetic Bragg reflections (first and second rows, respectively) for (a) $\text{La}_2\text{CoTiO}_6$ and (b) $\text{La}_2\text{NiTiO}_6$. Inset: Magnetic ordering described in the text.

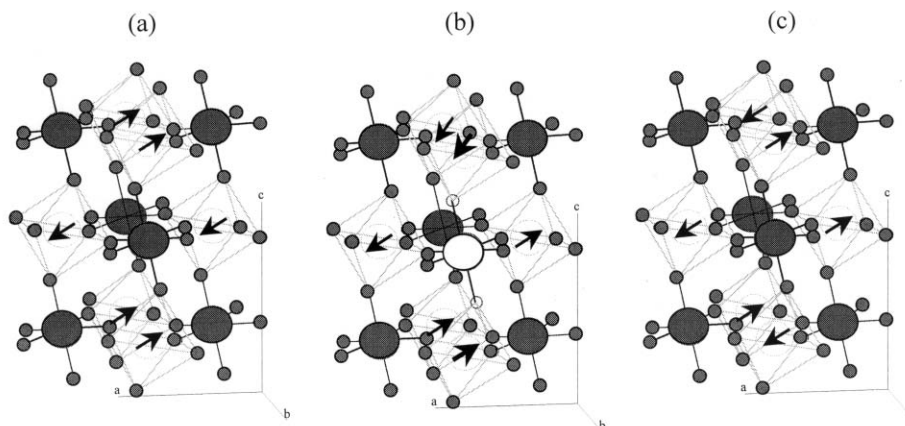


Fig. 7 The antiferromagnetic structures available to a monoclinic cell: (a) type I, (b) type II and (c) type III.

In the system La_2MTiO_6 there are three possible types of magnetic structures¹⁵ which are shown in Fig. 7 on the basis of a monoclinic unit cell.

There are two principal interactions in such structures:

(1) Those between the nn magnetic cations, separated by a distance of $\sqrt{2}a_p$ (corresponding to the a or b parameters), involving a path defined by M-O-O-M .

(2) And those between the nnn magnetic ions separated by $2a_p$ along the pathway of the form M-O-B-O-M , where B is a diamagnetic cation Ti^{4+} .

If the strength of the latter interaction is negligible, then the array of magnetic ions is expected to show a type I spin ordering, depicted in Fig. 7a. In this case, the nuclear and magnetic cell are the same and the coupling between paramagnetic ions are ferromagnetic in the a - c plane and antiferromagnetic between them along the c axis. This magnetic structure is similar to the A-type that was found for LaMnO_3 ³ where the paramagnetic ions are separated by a distance of a_p . However, if the strength of the nnn antiferromagnetic superexchange interactions is significant, but still less than the nn coupling, then a type III structure is predicted¹⁶ as shown in Fig. 7c. The magnetic cells are defined by the wave vector $\mathbf{k} = [\frac{1}{2}, \frac{1}{2}, \frac{1}{2}]$ and double a , b , and c axes relative to the monoclinic crystal cell should be considered. In this respect, LaCrO_3 ² and LaFeO_3 show a type G ordering which is the same as that described above. Finally, if the nnn interaction dominates, then type II ordering should occur, Fig. 7b. The wave vector $\mathbf{k} = [\frac{1}{2}, 0, \frac{1}{2}]$ characterizes the magnetic cell where double a and c axes are necessary. This is the spin ordering adopted by the title compounds, involving a path defined by M-O-Ti-O-M in which the oxygen atoms involved occupy the axial vertices of TiO_6 octahedra.

The existence of a strong superexchange interaction along the c direction is consistent with the $t_{2g}^5e_g^2$ and $t_{2g}^6e_g^2$ electron configurations of the octahedrally coordinated Co^{2+} and Ni^{2+} cations, respectively. However, in the compound SrLaNiSbO_6 ,¹⁰ a type I spin ordering was found because the strength of the nn interactions were the greatest. This can be explained by taking into account that the vacant 3d orbitals of Ti^{4+} are low enough in energy to take part in the superexchange process, whereas the 5p orbitals on Sb^{5+} have too high an energy to do so. A

similar behaviour of nn main interactions was reported for $\text{Sr}_2\text{HoRuO}_6$ ⁸ and $\text{Ba}_2\text{NdRuO}_6$,⁹ in which both B cations are paramagnetic, on the basis that the energies of the respective d-orbitals are too different to give rise to significant nnn interactions.

Acknowledgements

We are indebted to the CICYT (Grant MAT2000-1585-C03-02) for financial support. We acknowledge the ILL and CRG-D1B for collecting data of neutron diffraction.

References

- 1 C. N. R. Rao and B. Raveau, *Colossal Magnetoresistance, Charge Ordering and Related Properties of Manganese Oxides*, World Scientific, Singapore, 1998.
- 2 K. Tekuza, Y. Hinatsu, K. Oikawa, Y. Shimojo and Y. Morii, *J. Phys.: Condens. Matter*, 2000, **12**, 4151.
- 3 E. O. Wollan, *Phys. Rev.*, 1960, **117**(2), 387.
- 4 J. L. García-Muñoz, J. Rodríguez-Carvajal and P. Lacorre, *Phys. Rev., Sect. B*, 1994, **50**(2), 978.
- 5 M. L. Medarde, *J. Phys.: Condens. Matter*, 1997, **9**, 1679.
- 6 J. A. Alonso, J. L. García-Muñoz, M. T. Fernández-Díaz, M. A. G. Aranda, M. J. Martínez-Lope and M. T. Casais, *Phys. Rev. Lett.*, 1999, **82**(19), 3871.
- 7 P. D. Battle, T. C. Gibb, C. W. Jones and F. Studer, *J. Solid State Chem.*, 1989, **78**, 281.
- 8 Y. Izumiyama, Y. Doi, M. Wakeshima, Y. Hinatsu, K. Oikawa, Y. Shimojo and Y. Morii, *J. Mater. Chem.*, 2000, **10**, 2364.
- 9 Y. Doi, Y. Hinatsu, K. Oikawa, Y. Shimojo and Y. Morii, *J. Mater. Chem.*, 2000, **10**, 797.
- 10 M. P. Attfield, P. D. Battle, S. K. Bollen, T. C. Gibb and R. J. Whitehead, *J. Solid State Chem.*, 1992, **100**, 37.
- 11 M. Pechini, *US Patent*, 3,231,328, 1966.
- 12 E. Rodríguez, I. Alvarez, M. L. López, M. L. Veiga and C. Pico, *J. Solid State Chem.*, 1999, **148**, 479.
- 13 J. Rodríguez Carvajal, *Phys. A*, 1993, **192B**, 55.
- 14 A. I. Ruiz, M. L. López, M. L. Veiga and C. Pico, *J. Solid State Chem.*, 1999, **148**, 329.
- 15 P. D. Battle and C. W. Jones, *J. Solid State Chem.*, 1989, **78**, 108.
- 16 J. B. Goodenough, *Magnetism and the Chemical Bond*, Wiley, New York, 1963.